JOURNAL OF AGRICULTURAL AND FOOD CHEMISTRY
ARTICLE

J. Agric. Food Chem. **2009,** *57,* 10271–10281 **10271**
DOI:10.1021/jf900815x

Structural Characterization of the Lignin from Jute (*Corchorus capsularis*) Fibers

José C. del Río,*,† Jorge Rencoret,† Gisela Marques,† Jiebing Li,‡ Göran Gellerstedt,‡ Jesús Jiménez-Barbero,§ Ángel T. Martínez,§ and Ana Gutiérrez†

†Instituto de Recursos Naturales y Agrobiología de Sevilla (IRNAS), CSIC, PO Box 1052, E-41080 Seville, Spain, ‡Department of Fibre and Polymer Technology, Royal Institute of Technology (KTH), SE-100 44 Stockholm, Sweden, and §Centro de Investigaciones Biológicas (CIB), CSIC, Ramiro de Maeztu 9, E-28040 Madrid, Spain

The structural characteristics of the lignin from jute (*Corchorus capsularis*) fibers, which are used for high-quality paper pulp production, were studied. The lignin content (13.3% Klason lignin) was high compared to other nonwoody bast fibers used for pulp production. The lignin structure was characterized by pyrolysis-gas chromatography/mass spectrometry (Py-GC/MS), 2D-NMR, and thioacidolysis. Upon Py-GC/MS, jute fibers released predominantly products from syringylpropanoid units with the S/G ratio being 2.1 and a H/G/S composition of 2:33:65. 2D-NMR of the milled wood lignin (MWL) isolated from jute fibers showed a predominance of β-*O*-4′ aryl ether linkages (72% of total side chains), followed by β-β′ resinol-type linkages (16% of total side chains) and lower amounts of β-5′ phenylcoumaran (4%) and β-1′ spirodienone-type (4%) linkages and cinnamyl end groups (4%). The high predominance of the S-lignin units, together with the high proportion of β-*O*-4′ aryl ether linkages, which are easily cleaved during alkaline cooking, are advantageous for pulping. On the other hand, a small percentage (ca. 4%) of the lignin side chain was found to be acetylated at the γ-carbon, predominantly over syringyl units. The analysis of desulphurated thioacidolysis dimers provided additional information on the relative abundances of the various carbon−carbon and diaryl ether bonds and the type of units (syringyl or guaiacyl) involved in each of the above linkage types. Interestingly, the major part of the β-β′ dimers included two syringyl units, indicating that most of the β-β′ substructures identified in the HSQC spectra were of the syringaresinol type (pinoresinol being absent), as already observed in the lignin of other angiosperms.

KEYWORDS: Jute; *Corchorus capsularis*; nonwood fibers; pyrolysis-GC/MS; HSQC; thioacidolysis; milled wood lignin; syringyl; guaiacyl; syringaresinol

INTRODUCTION

Jute (*Corchorus capsularis*) is a herbaceous annual plant from the Tiliaceae family, mostly grown in Southeast Asian countries. Jute fiber is collected from the bast or outer region of the stem after retting of the whole plant and is a good source of different grades of pulp. There have been previous published studies describing the main characteristics of this interesting fiber (*1*) including some studies regarding jute pulping (*2*−*5*). However, little information is available concerning the composition and structural characteristics of the lignin from jute, whose content and composition are important parameters in pulp production in view of delignification rates, chemical consumption, and pulp yields (*6*, *7*).

In this paper, we report the composition and structural characteristics of the lignin from jute fibers. The lignin composition was characterized "in situ" by pyrolysis-gas chromatography−mass

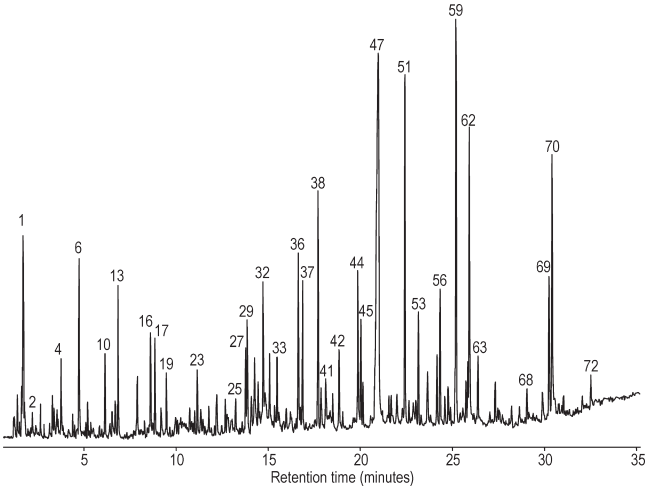

Figure 1. Py-GC/MS chromatogram of jute (*C. capsularis*) fibers. The identities and relative abundances of the released compounds are listed in **Table 1**.

*To whom correspondence should be addressed. Phone: +34-95-4624711. Fax: +34-95-4624002. E-mail: delrio@irnase.csic.es.

Published on Web 10/09/2009

Table 1. Composition and Relative Molar Abundances of the Compounds Released after Py-GC/MS of Jute Fibers[a]

No.	compound	mass fragments	MW	formula	origin	%
1	hydroxyacetaldehyde	42, 60	60	$C_2H_4O_2$	C	7.6
2	3-hydroxypropanal	73, 74	74	$C_3H_6O_2$	C	0.3
3	(3*H*)-furan-2-one	55, 84	84	$C_4H_4O_2$	C	0.1
4	2,3-butanedione	56, 57, 86	86	$C_4H_6O_2$		1.6
5	(2*H*)-furan-3-one	55, 84	84	$C_4H_4O_2$	C	0.5
6	furfural	67, 95, 96	96	$C_5H_4O_2$	C	3.4
7	2-methylfuran	53, 81, 82	82	C_5H_6O	C	0.3
8	2-(hydroxymethyl)furan	43, 70, 81, 98	98	$C_5H_6O_2$	C	0.7
9	cyclopent-1-ene-3,4-dione	54, 68, 96	96	$C_5H_4O_2$	C	0.2
10	4-methyltetrahydrofuran-3-one	43, 72	100	$C_5H_8O_2$	C	1.3
11	(5*H*)-furan-2-one	55, 84	84	$C_4H_4O_2$	C	0.8
12	acetylfuran	43, 95, 110	110	$C_6H_6O_2$	C	0.1
13	2,3-dihydro-5-methylfuran-2-one	55, 69, 98	98	$C_5H_6O_2$	C	2.9
14	5-methyl-2-furfuraldehyde	53, 109, 110	110	$C_6H_6O_2$	C	0.4
15	phenol	65, 66, 94	94	C_5H_6O	LH	0.2
16	5,6-dihydropyrane-2,5-dione	68, 98	98	$C_5H_6O_2$	C	2.0
17	4-hydroxy-5,6-dihydro-(2*H*)-pyran-2-one	58, 85, 114	114	$C_5H_6O_3$	C	1.7
18	3-hydroxy-2-methyl-2-cyclopenten-1-one	55, 84, 112	112	$C_6H_8O_2$	C	0.8
19	2-hydroxy-3-methyl-2-cyclopenten-1-one	55, 84, 112	112	$C_6H_8O_2$	C	1.2
20	2,3-dimethylcyclopenten-1-one	67, 110	110	$C_7H_{10}O$	C	0.1
21	4-methylphenol	77, 107, 108	108	C_7H_8O	LH	0.2
22	2-furoic acid, methyl ester	67, 95, 126	126	$C_6H_6O_3$	C	0.3
23	guaiacol	81, 109, 124	124	$C_7H_8O_2$	LG	1.1
24	4-ethylphenol	77, 107, 122	122	$C_8H_{10}O_2$	LH	0.1
25	3,4-dihydroxybenzaldehyde	81, 109, 137, 138	138	$C_7H_6O_3$	L	0.3
26	3,5-dihydroxy-2-methyl-(4*H*)-pyran-4-one	43, 68, 113, 142	142	$C_6H_6O_4$	C	0.2
27	5-hydroxymethyl-2-tetrahydrofuraldehyde-3-one	43, 57, 69, 70, 85	144	$C_6H_8O_4$	C	1.1
28	4-methylguaiacol	95, 123, 138	138	$C_8H_{10}O_2$	LG	0.6
29	catechol	64, 81, 92, 110	110	$C_6H_6O_2$	L/C	1.6
30	5-hydroxymethyl-2-furaldehyde (isomer)	69, 97, 126	126	$C_6H_6O_3$	C	0.9
31	4-vinylphenol	65, 91, 120	120	C_8H_8O	LH	0.2
32	5-hydroxymethyl-2-furaldehyde	69, 97, 126	126	$C_6H_6O_3$	C	2.2
33	3-methoxycatechol	79, 97, 125, 140	140	$C_7H_8O_3$	L	0.9
34	4-ethylguaiacol	122, 137, 152	152	$C_9H_{12}O_2$	LG	0.3
35	4-methylcatechol	78, 107, 123, 124	124	$C_7H_8O_2$	L	0.2
36	1,4-dideoxy-D-glycerohex-1-enopyranos-3-ulose	73, 87, 113, 144	144	$C_6H_8O_4$	C	3.0
37	4-vinylguaiacol	107, 135, 150	150	$C_9H_{10}O_2$	LG	2.0
38	syringol	111, 139, 154	154	$C_8H_{10}O_3$	LS	3.4
39	eugenol	131, 149, 164	164	$C_{10}H_{12}O_2$	LG	0.7
40	pyrogallol	52, 80, 97, 108, 126	126	$C_6H_6O_3$		0.2
41	3-methoxycatechol	79, 97, 125, 140	140	$C_7H_8O_3$	L	1.2
42	vanillin	109, 151, 152	152	$C_8H_8O_3$	LG	1.3
43	*cis*-isoeugenol	131, 149, 164	164	$C_{10}H_{12}O_2$	LG	0.1
44	4-methylsyringol	125, 153, 168	168	$C_9H_{12}O_2$	LS	2.1
45	*trans*-isoeugenol	131, 149, 164	164	$C_{10}H_{12}O_2$	LG	1.3
46	homovanillin	122, 137, 166	166	$C_{10}H_{14}O_2$	LG	0.7
47	levoglucosane	57, 60, 73, 98	162	$C_6H_{10}O_5$	C	19.6
48	4-ethylsyringol	167, 182	182	$C_{10}H_{14}O_3$	LS	0.2
49	guaiacylacetone	122, 137, 180	180	$C_{10}H_{12}O_3$	LG	0.2
50	1,6-anhydro-β-D-glucofuranose	73, 85, 115	162	$C_6H_{10}O_5$	C	0.7
51	4-vinylsyringol	137, 165, 180	180	$C_{10}H_{12}O_3$	LS	4.3
52	guaiacyl vinyl ketone	123, 151, 178	178	$C_{10}H_{10}O_3$	LG	0.4
53	4-allylsyringol	167, 179, 194	194	$C_{11}H_{14}O_3$	LS	1.3
54	4-propylsyringol	123, 167, 196	196	$C_{11}H_{16}O_3$	LS	0.1
55	*cis*-4-propenylsyringol	167, 179, 194	194	$C_{11}H_{14}O_3$	LS	1.0
56	syringaldehyde	167, 181, 182	182	$C_9H_{10}O_4$	LS	1.7
57	*cis*-coniferyl alcohol	124, 137, 151, 180	180	$C_{10}H_{12}O_3$	LG	0.4
58	4-propinylsyringol	106, 131, 177, 192	192	$C_{11}H_{12}O_3$	LS	0.6
59	*trans*-4-propenylsyringol	167, 179, 194	194	$C_{11}H_{14}O_3$	LS	5.4
60	acetosyringone	153, 181, 196	196	$C_{10}H_{12}O_4$	LS	0.4
61	*trans*-coniferaldehyde	107, 135, 147, 178	178	$C_{10}H_{10}O_3$	LG	0.5
62	*trans*-coniferyl alcohol	124, 137, 151, 180	180	$C_{10}H_{12}O_3$	LG	3.7
63	syringylacetone	123, 167, 210	210	$C_{11}H_{14}O_4$	LS	0.6
64	*cis*-coniferyl acetate	91, 103, 179, 222	222	$C_{12}H_{14}O_4$	LG	0.1
65	propiosyringone	151, 181, 210	210	$C_{11}H_{14}O_4$	LS	0.1
66	dihydrosinapyl alcohol	167, 168, 212	212	$C_{11}H_{16}O_4$	LS	0.6
67	*trans*-coniferyl acetate	91, 103, 179, 222	222	$C_{12}H_{14}O_4$	LG	0.1
68	*cis*-sinapyl alcohol	154, 167, 210	210	$C_{11}H_{14}O_4$	LS	0.4

Table 1. Continued

No.	compound	mass fragments	MW	formula	origin	%
69	*trans*-sinapaldehyde	137, 165, 180, 208	208	$C_{11}H_{12}O_4$	LS	1.8
70	*trans*-sinapyl alcohol	154, 167, 210	210	$C_{11}H_{14}O_4$	LS	3.1
71	*cis*-sinapyl acetate	149, 161, 209, 252	252	$C_{13}H_{16}O_5$	LS	0.1
72	*trans*-sinapyl acetate	149, 161, 209, 252	252	$C_{13}H_{16}O_5$	LS	0.3
	%H					2
	%G					32
	%S					66
	S/G					2.1

[a] C: carbohydrates; LH: *p*-hydroxyphenyl lignin units, H; LG: guaiacyl lignin units, G; LS: syringyl lignin units, S. Underlined mass fragments indicate base peaks.

spectrometry (Py-GC/MS), a rapid and highly sensitive technique for characterizing the chemical structure of lignin (*7*−*10*). In addition, for a more complete structural characterization, the milled-wood lignin (MWL) was isolated and analyzed by 2D-NMR spectroscopy and thioacidolysis. 2D-NMR provides information on the structure of the whole macromolecule and is a powerful tool for lignin structural characterization, revealing both the aromatic units and the different interunit linkages present in the lignin polymer (*11*−*17*). On the other hand, thioacidolysis is a selective method that degrades the most frequent interunit linkage in lignin, that is, the β-*O*-4′ ether linkage. The total yields and relative distribution of the thioacidolysis monomers reflect the amount and ring type of lignin units involved in these alkyl−aryl ether bonds. In addition, the dimers recovered after thioacidolysis can provide information about the units involved in the various carbon−carbon and diaryl ether linkages, often referred to as the "condensed" bonds (including 5-5′, 4-*O*-5′, β-1′, β-5′ and β-β′) (*16*, *18*−*20*).

The knowledge of the structure of the lignin polymer of jute fibers will help to maximize the exploitation of this interesting fiber for pulp and paper production.

MATERIALS AND METHODS

Samples. Jute (*C. capsularis*) fibers were supplied by CELESA pulp mill (Tortosa, Spain). Jute fibers were air-dried. The dried samples were milled using a knife mill (Janke and Kunkel, Analysenmühle) and successively extracted with acetone (in a Soxhlet apparatus for 8 h) and hot water (3 h at 100 °C). Klason lignin content was estimated as the residue after sulphuric acid hydrolysis of the pre-extracted material according to Tappi rule T222 om-88 (*21*). The acid-soluble lignin was determined, after the insoluble lignin was filtered off, by UV-spectroscopic determination at 205 nm wavelength. Ash content was estimated as the residue after 6 h of heating at 575 °C. Two replicates were used for each sample. The immediate analysis of jute fibers (as percent of whole fiber) is as follows: ash, 1.0%; acetone extractives, 0.4%; water-soluble material, 1.0%; Klason lignin, 13.3%; acid-soluble lignin, 2.8%.

Lignin Isolation. MWL was extracted from finely ball-milled (ca. 100 h) plant material, free of extractives and hot water-soluble material, using dioxane−water (9:1, v/v), followed by evaporation of the solvent, and purified as described (*22*). The final yield was around 20% of the original lignin content.

Analytical Pyrolysis. Py-GC/MS of jute fibers was performed in duplicate with a Curie-point pyrolyser (Horizon Instruments Ltd.) coupled to a Varian Saturn 2000 GC/MS, using a 30 m × 0.25 mm i.d., 0.25 μm DB-5 column. Approximately 100 μg of finely divided sample was deposited on a ferromagnetic wire, then inserted into the glass linear, and immediately placed in the pyrolyser. The pyrolysis was carried out at 610 °C. The chromatograph was programmed from 40 °C (1 min) to 300 °C at a rate of 6 °C/min. The final temperature was held for 20 min. The injector, equipped with a liquid carbon dioxide cryogenic unit, was programmed from −30 °C (1 min) to 300 °C at 200 °C/min, while the GC/MS interface was kept at 300 °C. The compounds were identified by comparing the mass spectra obtained with those of the Wiley and NIST computer libraries and those reported in the literature (*8*, *9*). Relative peak molar areas were calculated for carbohydrate and lignin pyrolysis products. The summed molar areas of the relevant peaks were normalized to 100% and the data for two repetitive pyrolysis experiments were averaged.

NMR Spectroscopy. NMR spectrum of jute MWL was recorded at 25 °C on a Bruker AVANCE 500 MHz equipped with a *z*-gradient triple resonance probe. Around 40 mg of jute MWL were dissolved in 0.75 mL of deuterated dimethylsulfoxide (DMSO-d_6) and 2D-NMR spectra were recorded in HSQC (heteronuclear single quantum correlation) experiments. The spectral widths were 5000 and 13200 Hz for the ^{1}H- and ^{13}C-dimensions, respectively. The number of collected complex points was 2048 for ^{1}H-dimension with a recycle delay of 5 s. The number of transients was 64, and 256 time increments were always recorded in ^{13}C-dimension. The $^1J_{CH}$ used was 140 Hz. The *J*-coupling evolution delay was set to 3.2 ms. Squared cosine-bell apodization function was applied in both dimensions. Prior to Fourier transformation, the data matrixes were zero filled up to 1024 points in the ^{13}C-dimension. The central solvent peak was used as an internal reference (δ_C 39.5; δ_H 2.50). HSQC cross-signals were assigned by comparing with the literature (*11*−*17*, *23*). A semiquantitative analysis of the intensities of the HSQC cross-signal was performed (*24*, *25*). Because the cross-signal intensity depends on the particular $^1J_{CH}$ value, as well on the T_2 relaxation time, a direct analysis of the intensities is impossible. Thus, the integration on the cross-signals was performed separately for the different regions of the HSQC spectrum, which contain signals that correspond to chemically analogous carbon-proton pairs. For these signals, the $^1J_{CH}$ coupling value is relatively similar and can be used semiquantitatively to estimate the relative abundance of the different species. In the aliphatic oxygenated region, the relative abundance of side chains involved in interunit linkages were estimated from the C_α−H_α correlations to avoid possible interference from homonuclear ^{1}H−^{1}H couplings. In the aromatic region, C−H correlations from S and G units were used to estimate the lignin S/G ratio.

Thioacidolysis. Thioacidolysis of 5 mg of MWL was performed as described by Rolando et al. (*20*) using 0.2 M BF_3 etherate in dioxane/ethanethiol 8.75:l. The reactions products were extracted with CH_2Cl_2, dried, and concentrated. GC analysis of trimethylsilylated (using *N*,*O*-bis-(trimethylsilyl)-trifluoroacetamide, BSTFA) samples was performed with a Hewlett-Packard 6890 instrument using an Rtx 5 column from Restec Corporation (45 m × 0.32 μm i.d., 0.25 μm film thickness) and a flame detector. The temperature was programmed from 180 to 270 °C (15 min) at 40 °C/min and then to 300 °C (5 min) at 4 °C/min. Injector and detector were at 250 and 280 °C, respectively, and He was the carrier gas.

Desulphuration of Thioacidolysis Degradation Products. A total of 200 μL of the CH_2Cl_2 solution containing the thioacidolysis products was desulphurated as described by Lapierre et al. (*18*). GC/MS analysis of the dimeric compounds was performed in a Varian Star 3400 equipment coupled to an ion-trap detector Varian Saturn 2000, using a DB-5HT fused-silica capillary column from J&W Scientific (30 m × 0.25 mm i.d., 0.1 μm film thickness). The temperature was programmed from 50 to 110 °C at 30 °C/min and then to 320 °C (13 min) at 6 °C/min. The injector and transfer line were at 300 °C. Trimeric compounds were analyzed using a short (12 m) capillary column of the same characteristics, a Varian 3800 chromatograph coupled to an ion-trap detector Varian 4000 (with a range up to 1000 *m*/*z*), and a temperature program from 60 °C (1 min) to 380 °C (5 min) at 10 °C/min. The transfer line was at 300 °C, and the injector was

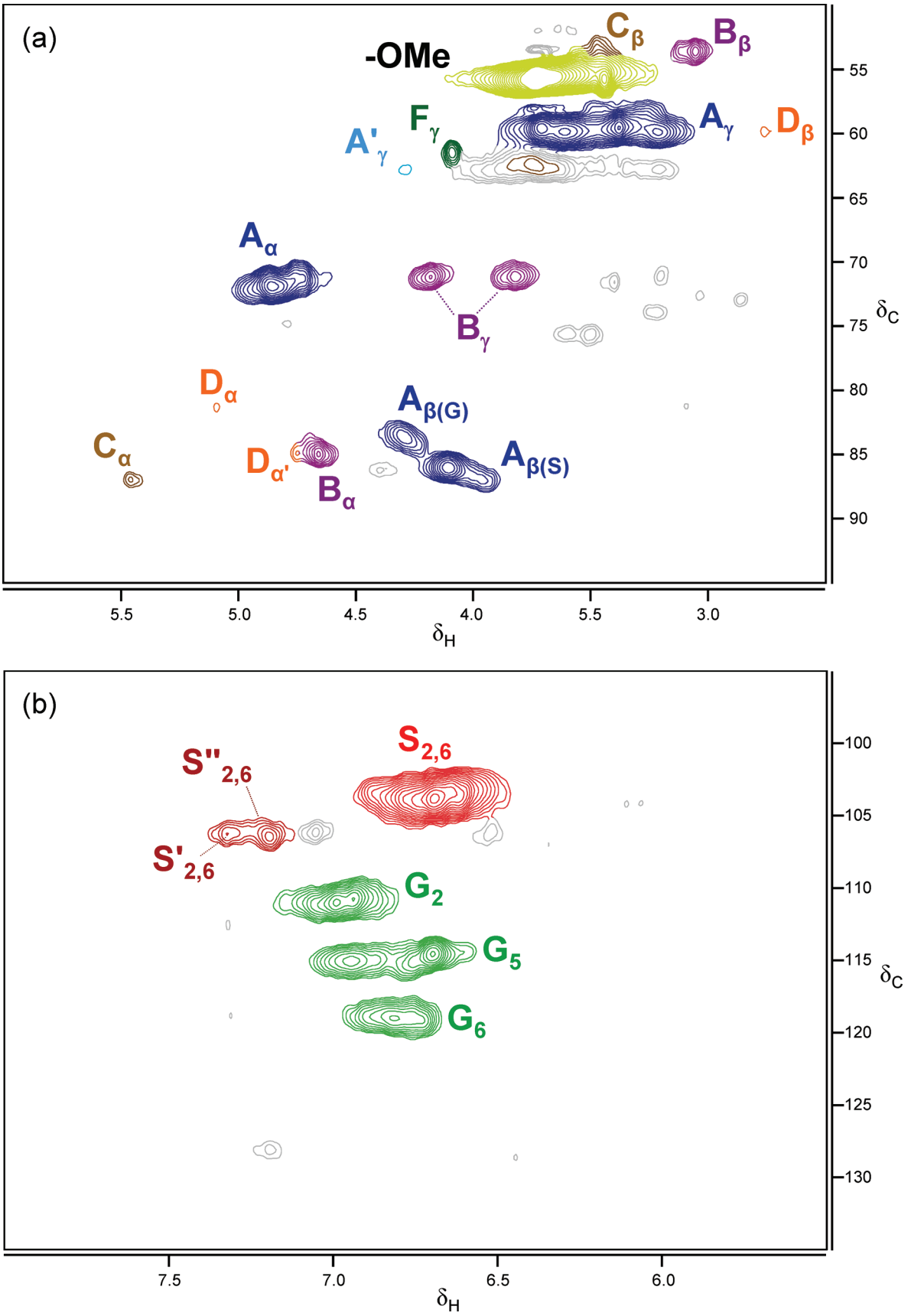

Figure 2. HSQC NMR spectrum of the MWL isolated from jute (*C. capsularis*) fibers: (a) expanded side chain region δ_C/δ_H 50−95/2.5−6.0 and (b) expanded aromatic region δ_C/δ_H 95−135/5.5−8.0. See **Table 2** for signal assignment and **Figure 3** for the main lignin structures identified.

programmed from 120 °C (0.1 min) to 380 at 200 °C/min. In both analyses, He was the carrier gas (2 mL/min) and tetracosane was used as internal standard. Dimer identification was based on previously reported mass spectra (*16*, *18*) and mass fragmentography.

Table 2. Assignments of $^{13}C-^{1}H$ Correlation Signals in the 2D-NMR Spectra of the MWL Isolated from Jute (*C. capsularis*) Fibers[a]

label	δ_C/δ_H (ppm)	assignment
C_β	53.5/3.46	$C_\beta-H_\beta$ in phenylcoumaran substructures (**C**)
B_β	53.5/3.06	$C_\beta-H_\beta$ in resinol substructures (**B**)
-OMe	55.6/3.73	C−H in methoxyls
A_γ	59.4 /3.40 and 3.72	$C_\gamma H_\gamma$ in β-*O*-4′ substructures (**A**)
D_β	59.6/2.75	$C_\beta-H_\beta$ in spirodienone substructures (**D**)
F_γ	61.3/4.09	$C_\gamma H_\gamma$ in *p*-hydroxycinnamyl alcohol end groups (**F**)
A'_γ	62.7/4.29	$C_\gamma H_\gamma$ in γ-acetylated β-*O*-4′ substructures (**A′**)
$A_{\alpha(G)}$	71.0/4.74	$C_\alpha-H_\alpha$ in β-*O*-4′ substructures linked to a G unit (**A**)
B_γ	71.0/3.83 and 4.19	$C_\gamma H_\gamma$ in resinol substructures (**B**)
A_α	71.7/4.86	$C_\alpha-H_\alpha$ in β-*O*-4′ substructures linked to a S unit (**A**)
D_α	81.2/5.09	$C_\alpha-H_\alpha$ in spirodienone substructures (**D**)
$A_{\beta(G)}$	83.5/4.28	$C_\beta-H_\beta$ in β-*O*-4′ substructures linked to a G unit (**A**)
B_α	84.8/4.67	$C_\alpha-H_\alpha$ in resinol substructures (**B**)
D_α'	84.8/4.75	$C_\alpha'-H_\alpha'$ in spirodienone substructures (**D**)
$A_{\beta(S)}$	85.8/4.11	$C_\beta-H_\beta$ in β-*O*-4′ substructures linked to a S unit (**A**)
C_α	86.8/5.46	$C_\alpha-H_\alpha$ in phenylcoumaran substructures (**C**)
$S_{2,6}$	103.8/6.69	$C_{2,6}-H_{2,6}$ in etherified syringyl units (**S**)
$S'_{2,6}$	106.1/7.32	$C_{2,6}-H_{2,6}$ in oxidized (C_α=O) phenolic syringyl units (**S′**)
$S''_{2,6}$	106.4 /7.19	$C_{2,6}-H_{2,6}$ in oxidized (C_αOOH) syringyl units (**S″**)
G_2	110.9/6.99	C_2-H_2 in guaiacyl units (**G**)
G_5	114.9/6.72 and 6.94	C_5-H_5 in guaiacyl units (**G**)
G_6	118.7/6.77	C_6-H_6 in guaiacyl units (**G**)

[a] Signals were assigned by comparing with the literature (*11*−*17*, *23*).

RESULTS AND DISCUSSION

Jute fibers presented a lignin content (estimated as Klason lignin) of 13.3% of the total fiber that amounted up to 16.1% by taking into account the acid-soluble lignin, in agreement with previous studies (*1*, *4*, *5*). This lignin content is higher than that in other nonwood bast fibers used for papermaking such as hemp or flax, with a lignin content less than 5% (*26*−*29*), although it is comparable to that reported for kenaf bast fiber (*30*). The composition of the lignin in jute fibers was first analyzed by Py-GC/MS, which allows for the rapid characterization of the lignin in terms of its H/G/S composition. Then, for a more detailed structural characterization, the MWL was isolated by aqueous dioxane extraction from finely ball-milled wood according to the classical lignin isolation procedure (*22*) and subsequently analyzed by 2D-NMR and thioacidolysis.

Py-GC/MS. The chemical composition of the lignin in jute fibers was analyzed in situ, without prior isolation, by Py-GC/MS. The Py-GC/MS chromatogram is shown in **Figure 1**, and the identities and relative abundances of the released compounds are listed in **Table 1**. The compounds released arise mainly from the carbohydrate and lignin moieties. Among the carbohydrate-derived compounds, the main ones are hydroyacetaldehyde (**1**), furfural (**6**), 2,3-dihydro-5-methylfuran-2-one (**13**), 4-hydroxy-5,6-dihydro-(2*H*)-pyran-2-one (**17**), 5-hydroxymethyl-2-furfuraldehyde (**32**), 1,4-dideoxy-D-glycerohex-1-enopyranos-3-ulose (**36**), and levoglucosane (**30**). Among the lignin-derived phenols, the pyrogram of jute fibers showed compounds derived from guaiacyl (G) and syringyl (S) lignin units. Compounds derived from *p*-hydroxyphenyl (H) lignin units were found in minor amounts (2% of typical lignin-derived compounds). The main lignin derived compounds released were guaiacol (**23**), 4-methylguaiacol (**28**), 4-vinylguaiacol (**37**), syringol (**38**), *trans*-isoeugenol (**46**), 4-methylsyringol (**45**), 4-vinylsyringol (**53**), 4-allylsyringol (**55**), *cis*- and *trans*-4-propenylsyringol (**57**, **61**), syringaldehyde (**58**), *trans*-coniferyl alcohol (**64**), *trans*-sinapaldehyde (**71**), and *trans*-sinapyl alcohol (**72**).

The lignin-derived S-type phenols were present in higher abundances than the respective G-type phenols, with a H/G/S composition of 2:32:66 and a S/G ratio of 2.1, in agreement with previous studies (*1*, *5*). The high lignin S/G ratio observed in jute lignin is comparable to those observed in hardwood lignins (*16*, *31*). Some bast fibers commonly used for pulp and papermaking, such as flax or hemp, have very low lignin S/G ratios (0.8 and 0.3, respectively) (*10*, *29*), although a high S/G ratio has also been found in another bast fiber, such as kenaf (*10*, *30*). The high S-lignin content observed in jute fibers is advantageous for delignification during pulping due to the higher reactivity of the S-lignin in alkaline systems (*32*, *33*). In general, the efficiency of pulping is directly proportional to the amount of syringyl (S) units in lignin. The guaiacyl (G) units have a free C-5 position available for carbon−carbon interunit bonds, which make them fairly resistant to lignin depolymerization during pulping. Higher S/G ratios imply higher delignification rates, less alkali consumption and therefore higher pulp yield (*6*, *7*).

A detailed analysis of the compounds released after Py-GC/MS of jute fibers revealed the presence of sinapyl acetate, in *cis* and *trans* forms (peaks **71** and **72**, respectively). Minor amounts of coniferyl acetates (*cis* and *trans* forms, peaks **64** and **67**, respectively) were also detected. Acetylated lignin units have already been reported to occur in the pyrolysates of other fibers (kenaf, abaca, sisal) (*10*) and indicates that jute lignin is, at least partially, acetylated at the γ-carbon of the side chain. Recent studies using a modification of the so-called derivatization followed by reductive cleavage (DFRC) method, developed by Ralph and Lu (*34*), indicated that jute lignin is slightly acetylated, and preferentially over the syringyl units (6.4% acetylated S-units and only 0.3% acetylated G-units) (*35*). This contrasts with the lignin from the bast fibers of kenaf, a related plant from the Malvales, that is extensively acetylated (up to 60% of S-lignin) (*17*, *35*).

2D-NMR. For a more complete structural characterization of jute lignin, the MWL of jute fibers was isolated and subjected to 2D-NMR analysis. The HSQC NMR spectrum of jute MWL showed three regions corresponding to aliphatic, side chain, and aromatic $^{13}C-^{1}H$ correlations. The aliphatic (nonoxygenated) region showed signals with no structural information and therefore is not discussed in detail. The side chain (δ_C/δ_H 50−95/2.5−6.0) and the aromatic (δ_C/δ_H 95−135/5.5−8.0) regions of the HSQC spectrum of jute MWL are shown in **Figure 2**. The main

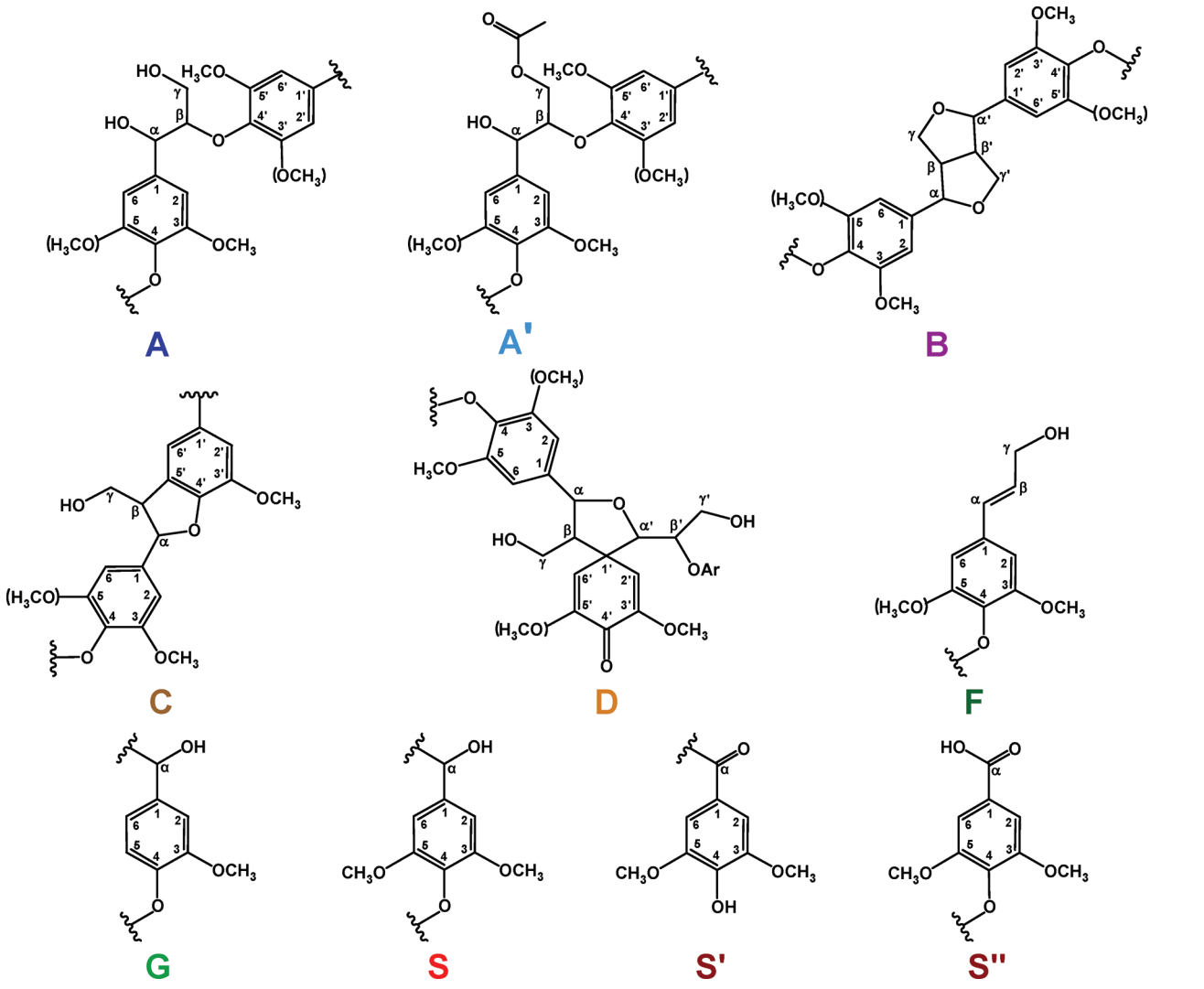

Figure 3. Main structures present in jute (*C. capsularis*) lignin: (**A**) β-*O*-4′ linkages; (**A′**) β-*O*-4′ linkages with acetylated γ-carbon; (**B**) resinol structures formed by β-β'/α-*O*-γ'/γ-*O*-α' linkages; (**C**) phenylcoumarane structures formed by β-5′/α-*O*-4′ linkages; (**D**) spirodienone structures formed by β-1′/α-*O*-4′ linkages; (**F**) *p*-hydroxycinnamyl alcohol end groups; (**G**) guaiacyl unit; (**S**) syringyl unit; (**S′**) oxidized syringyl unit bearing a carbonyl group at Cα (phenolic); (**S″**) oxidized syringyl unit bearing a carboxyl group at Cα.

Table 3. Structural Characteristics (Relative Abundance of the Main Inter-Unit Linkages, Percentage of γ-Acylation and S/G Ratio) from Integration of $^{13}C-^{1}H$ Correlation Signals in the HSQC Spectra of the MWL from Jute (*C. capsularis*) Fibers

linkage relative abundance (% of side chains involved)	
β-*O*-4′ linked units (**A**/**A′**)	72
resinols (**B**)	16
phenylcoumarans (**C**)	4
spirodienones (**D**)	4
p-hydroxycinnamyl alcohols (**F**)	4
erythro/*threo* ratio in β-*O*-4′ units	3.5
percentage of γ-acetylation	4
S/G ratio	2.0

lignin cross-signals assigned in the HSQC spectrum are listed in **Table 2** and the main substructures found are depicted in **Figure 3**.

The side chain region of the spectrum (**Figure 2**a) gave useful information about the different interunit linkages present in jute lignin. The spectrum showed prominent signals corresponding to β-*O*-4′ ether linkages (substructure **A**). The $C_\alpha-H_\alpha$ correlations in β-*O*-4′ substructures were observed at δ_C/δ_H 71.0/4.74 and 71.7/4.86 for structures linked to G or S lignin units, respectively. Likewise, the $C_\beta-H_\beta$ correlations were observed at δ_C/δ_H

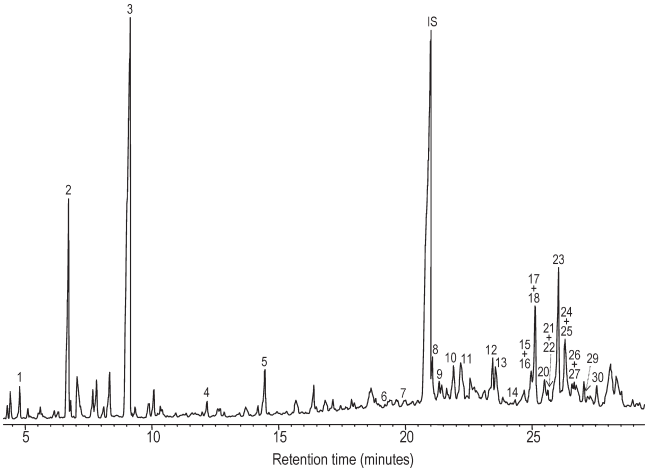

Figure 4. Chromatogram of the thioacidolysis degradation products (after Raney-nickel desulphuration) released from jute MWL, as trimethylsilyl derivatives. The numbers refer to the compounds (monomers and dimers) listed in **Table 4** and the structures are shown in **Figure 5**. IS refers to tetracosane used as internal standard.

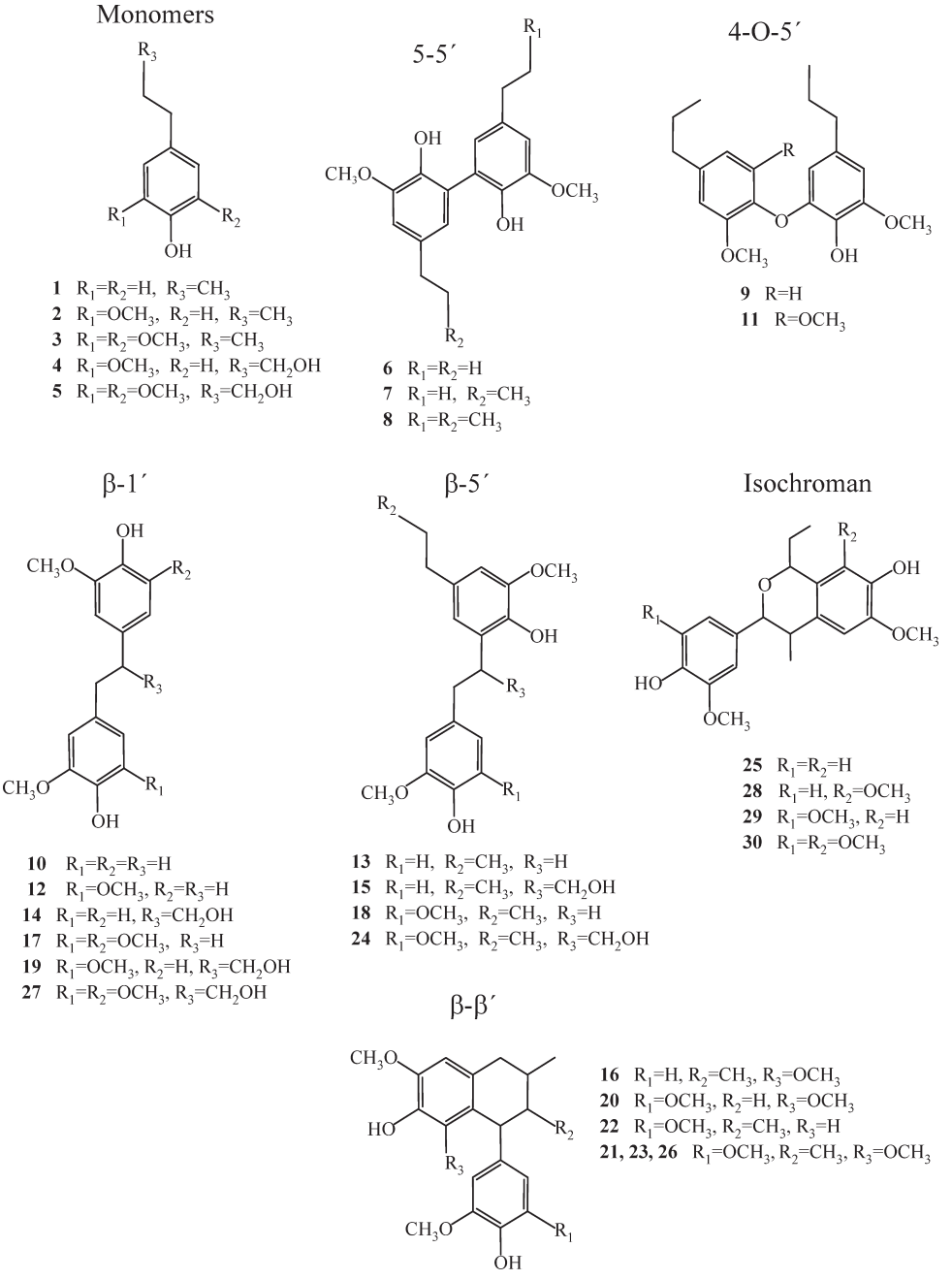

Figure 5. Structures of monomeric and dimeric compounds obtained after thioacidolysis and Raney-nickel desulphuration of the jute MWL. The mass spectral data of the compounds (as trimethylsilyl derivatives) are listed in **Table 4**.

85.8/4.11 in *β-O-4′* substructures linked to an S-lignin unit and at δ_C/δ_H 83.5/4.28 in *β-O-4′* substructures linked to a G-lignin unit. Moreover, the $C_\beta-H_\beta$ correlations corresponding to the *erythro* and *threo* forms of the S-type *β-O-4′* substructures can be distinguished at δ_C/δ_H 85.8/4.11 and 86.8/3.96, respectively. The $C_\gamma-H_\gamma$ correlations in *β-O-4′* substructures were observed at δ_C/δ_H 59.4/3.40 and 3.72, partially overlapped with other signals. Interestingly, a small but clear signal was observed at δ_C/δ_H 62.7/4.29, corresponding to the $C_\gamma-H_\gamma$ correlations in γ-acetylated lignin units (**A′**). This signal indicates that the lignin from jute is partially acetylated at the γ-carbon of the side chain, as shown above and in agreement with previous studies (*10*, *35*). The percentage of acetylation of the lignin side chain was estimated from the $C_\gamma-H_\gamma$ correlations and accounted for about 4%, which is in close agreement with the DFRC results (*35*).

In addition to *β-O-4′* substructures, other linkages were also observed. Strong signals for resinol (*β-β′*/α-*O*-γ′/γ-*O*-α′) substructures (**B**) were observed in the spectrum, with their $C_\alpha-H_\alpha$, $C_\beta-H_\beta$ and the double $C_\gamma-H_\gamma$ correlations at δ_C/δ_H 84.8/4.67, 53.5/3.06 and 71.0/3.83 and 4.19, respectively. Phenylcoumaran (*β-5′*/α-*O*-4) substructures (**C**) were also found although in lower amounts, the signals for their $C_\alpha-H_\alpha$ and $C_\beta-H_\beta$ correlations being observed at δ_C/δ_H 86.8/5.46 and 53.5/3.46, respectively, and that of $C_\gamma-H_\gamma$ correlation overlapping with other signals around δ_C/δ_H 62/3.8. Finally, small signals corresponding to spirodienone (*β-1′*/α-*O*-α′) substructures (**D**) could also be observed in the spectrum, their $C_\alpha-H_\alpha$, $C_{\alpha'}-H_{\alpha'}$, and $C_\beta-H_\beta$ correlations being at δ_C/δ_H 81.2/5.09, 84.8/4.75, and 59.6/2.75, respectively. Other small signals in the side chain region of the HSQC spectrum of jute MWL corresponded to $C_\gamma-H_\gamma$ correlations (at δ_C/δ_H 61.3/4.09) assigned to *p*-hydroxycinnamyl (**F**) end groups. Signals

Table 4. Identification, Mass Spectral Fragments, and Relative Molar Abundances of the Compounds (Silylated Monomers and Dimers) Released after Thioacidolysis and Raney-Nickel Desulphuration of Jute MWL[a]

compound	linkage	fragments (*m*/*z*)	M_w	relative abundance (%)
		Monomers		
1	H	208, 193, 179	208	2
2	G	238, 223, 209, 179, 73	238	22
3	S	268, 253, 239,238, 209	268	71
4	G-OH	326, 311, 236, 206, 179	326	1
5	S-OH	356, 341, 240	356	4
			H/G/S (from monomers)	2:23:75
		Dimers		
6	5-5′ (G-G)	446, 431, 417, 416, 73	446	0.7
7	5-5′ (G-G)	460, 445, 431, 430, 73	460	1.0
8	5-5′ (G-G)	474, 459, 445, 444, 385, 357, 73	474	8.5
9	4-*O*-5′ (G-G)	402, 387, 373, 372, 357, 343, 73	402	3.8
10	*β*-1′ (G-G)	418, 209, 179, 73	418	2.4
11	4-*O*-5′ (G-S)	432, 417, 403, 73	432	7.6
12	*β*-1′ (G-S)	448, 433, 239, 209, 179, 73	448	3.6
13	*β*-5′ (G-G)	460, 445, 251, 236, 209, 207,179, 73	460	2.6
14	*β*-1′ (G-G,-OH)	520, 505, 417, 311, 223, 209, 179, 149, 73	520	0.1
15	*β*-5′ (G-G,-OH)	562, 472, 352, 263, 209, 191, 73	562	4.1
16	*β*-*β*′ (G-S)	502, 306, 269, 239, 209, 73	502	3.2
17	*β*-1′ (S-S)	478, 463, 239, 209, 73	478	8.4
18	*β*-5′ (G-S)	490, 239, 209, 73	490	12.3
19	*β*-1′ (G-S,-OH)	550, 535, 341, 73	550	0.1
20	*β*-*β*′ (S-−S)	518, 503, 489, 488, 292, 73	518	5.6
21	*β*-*β*′ (S-S)	532, 517, 502, 445, 306, 291, 275, 73	532	2.1
22	*β*-*β*′ (G-S)	502, 487, 472, 415, 276, 73	502	1.3
23	*β*-*β*′ (S-S)	532, 517, 502, 445, 306, 291, 275, 73	532	22.6
24	*β*-5′ (G-S,-OH)	592, 502, 472, 239,209, 191, 73	592	4.7
25	*β*-1′/α-*O*-α′ (G-G)	488, 473, 459, 279, 251, 209, 73	488	1.3
26	*β*-*β*′ (S-S)	532, 517, 502, 445, 306, 291, 275, 73	532	0.8
27	*β*-1′ (S-S,-OH)	580, 565, 341, 239, 209, 73	580	0.2
28	*β*-1′/α-*O*-α′ (G-S)	518, 503, 489, 309, 239, 209, 73	518	0.9
29	*β*-1′/α-*O*-α′ (S-G)	518, 503, 489, 279, 251, 239, 209, 73	518	2.1
30	*β*-1′/α-*O*-α′ (S-S)	548, 533, 519, 309, 278, 281, 239, 209, 73	548	0.7

[a] Their structures are depicted in **Figure 5**.

corresponding to dibenzodioxocin structures could not be observed in the HSQC spectrum of jute MWL, as corresponds to a lignin enriched in S-units.

The main cross-signals in the aromatic region of the HSQC spectrum (**Figure 2**b) corresponded to the benzenic rings of the different lignin units. Signals from syringyl (**S**) and guaiacyl (**G**) units were observed. The S-lignin units showed a prominent signal for the $C_{2,6}-H_{2,6}$ correlation at δ_C/δ_H 103.8/6.69, while the G-lignin units showed different correlations for C_2-H_2 (δ_C/δ_H 110.9/6.99), C_5-H_5 (δ_C/δ_H 114.9/6.72 and 6.94), and C_6-H_6 (δ_C/δ_H 118.7/6.77). The double C_5-H_5 signal revealed some heterogeneity among the G units especially affecting the C_5-H_5 correlation, probably because it is due to different substituents at C_4 (e.g., phenolic or etherified in different substructures). Signals corresponding to $C_{2,6}-H_{2,6}$ correlations in C_α-oxidized S-lignin units (**S**′ and **S**′) were observed at δ_C/δ_H 106.1/7.32 and 106.4/7.19, respectively. However, signals of H-lignin units were not detected in the HSQC spectrum of jute MWL, in agreement with the low abundance of these units observed by Py-GC/MS (2% of H-units). The NMR estimation of the lignin S/G ratio accounts for 2.0, similar to that observed by Py-GC/MS.

The relative abundances of the main interunit linkages present in the jute MWL, as well as the percentage of *γ*-acetylation and the molar S/G ratios, calculated from the HSQC spectrum, are shown in **Table 3**. The data indicated that the structure of jute lignin is similar to a hardwood lignin, with a high S/G ratio, a predominance of *β*-*O*-4′ aryl ether linkages (72% of total side chains), followed by *β*-*β*′ resinol-type linkages (16% of total side chains) and lower amounts of *β*-5′ phenylcoumaran (4%), *β*-1′ spirodienone-type (4%) linkages, and cinnamyl end groups (4%). It is interesting to note that no traces of *β*-*β*′ resinol (despite being the most abundant condensed structure) and *β*-1′ spirodienone-type linkages were detected in jute lignin in previous works (*1*). Moreover, a small percentage (ca. 4%) of the lignin side chain was found to be acetylated at the *γ*-carbon, predominantly over syringyl units. Finally, a predominance of the *erythro* over the *threo* diasteroisomers (*erythro*/*threo* ratio of ca. 3.5) was observed in *β*-*O*-4′ structures, in agreement with previous work (*1*) and with the tendency of S-lignin to favor the formation of the *erythro* isomers (*36*, *37*).

Table 5. Relative Molar Percentages of the Different Dimer Types (see **Table** 4 and **Figure** 5) Released after Thioacidolysis and Raney-Nickel Desulphuration of Jute MWL

5-5′	4-*O*-5′		*β*-1′			*β*-5′		*β*-*β*′		*β*-1′/α-*O*-α′		
GG	GG	SG	GG	SG	SS	GG	SG	SG	SS	GG	SG	SS
10	4	8	2	4	9	7	17	4	31	1	1	2

The high predominance of the S-lignin units, together with the high predominance of *β*-*O*-4′ aryl ether linkages, which are easily cleaved during alkaline cooking, are advantageous for pulping. Moreover, it has been suggested that the *erythro* form of *β*-*O*-4′

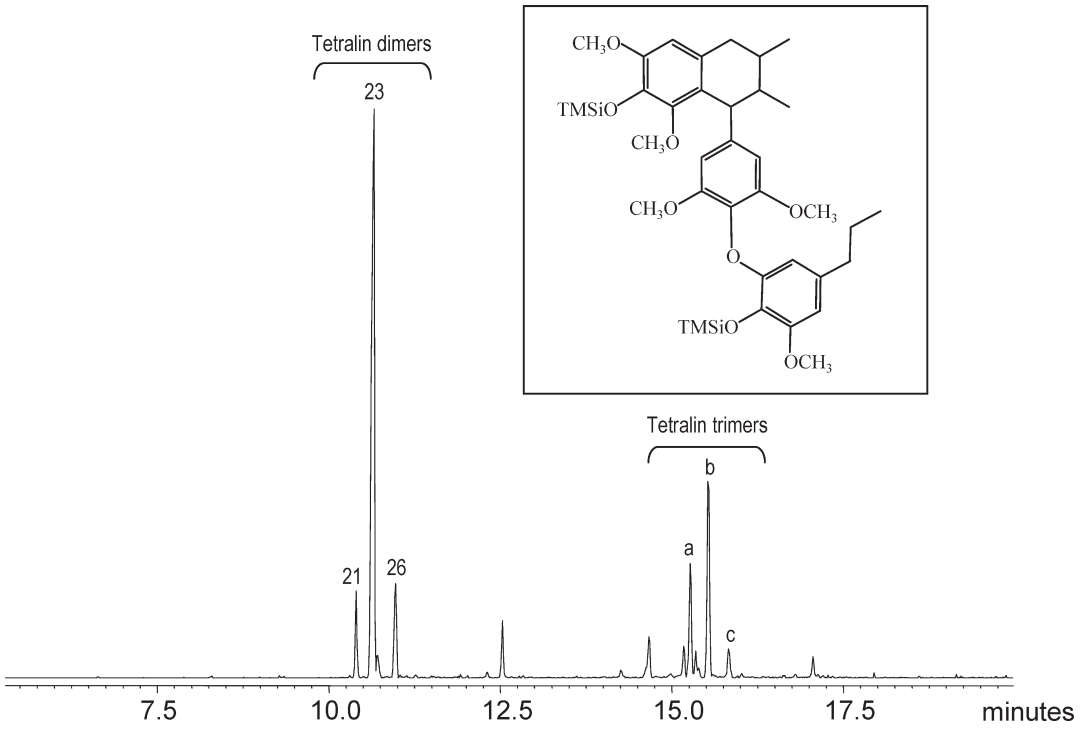

Figure 6. Reconstructed ion chromatogram (sum of ions at *m*/*z* 532 and *m*/*z* 696, characteristics of the tetralin dimers and trimers, respectively) of the thioacidolysis products (after Raney-nickel desulphuration) of jute MWL, as trimethylsilyl derivatives, showing the three isomers of the main tetralin dimers (peaks **21**, **23**, and **26**) and the three isomers of their corresponding trimeric compounds (**a**, **b**, and **c**). The chemical structure of the trimers is shown in the inset.

structures is removed more rapidly in pulping that the *threo* form (*13*, *38*, *39*). The high *erythro*/*threo* ratio observed is therefore advantageous for pulping.

Thioacidolysis. The MWL from jute fibers was also studied by thioacidolysis. The thioacidolysis degradation products were subjected to a Raney-nickel desulphuration and the products obtained were analyzed by GC/MS. The chromatogram of the trimethylsilylated products is shown in **Figure 4**. The compounds were identified according to previously reported mass spectra (*16*, *18*). The structures of the main compounds identified are shown in **Figure 5**, and their mass spectral data and relative abundances are summarized in **Table 4**.

The composition of the main monomers released after thioacidolysis showed a predominance of S over G units in the etherified jute lignin, a low abundance of H units (ca. 2%), and a H/G/S composition of 2:23:75. As expected, the molar S/G ratio obtained, 3.2, is higher than that estimated from Py-GC/MS and NMR, because the relative distribution of the thioacidolysis monomers reflect only the lignin units involved in β-*O*-4′ alkyl-aryl ether bonds.

On the other hand, the dimers recovered after thioacidolysis can provide useful information about the different units involved in the various carbon−carbon and diaryl ether linkages, often referred to as the "condensed" bonds (including 5-5′, 4-*O*-5′, β-1′, β-5′, and β-β′) (*18*, *19*). The main dimers identified were of 5-5′ (dimers **6**−**8**), 4-*O*-5′ (**9** and **11**), β-1′ (**10**, **12**, **14**, **17**, **19**, and **27**), β-5′ (**13**, **15**, **18**, and **24**), β-β′ tetralin (**13**, **20**−**23**, and **26**), and phenylisochroman (**25**, **28**−**30**; including β-1′/α-*O*-α′ bonds) types. The origin of the dimers can be established as follows: (i) the 5-5′ dimers arise mainly from breakdown of α-*O*-4′ and β-*O*-4′ ethers in dibenzodioxocins and from other 5-5′ biphenyl structures; (ii) the β-1′ dimers arise from breakdown of α-*O*-α′ ether and side chain lost in spirodienones; (iii) the β-5′ dimers arise from breakdown of α-*O*-4′ ether in phenylcoumaran substructures; and (iv) the β-β′ tetralin dimers arise from breakdown of two α-*O*-ether bonds in the pinoresinols and syringaresinols produced by the thioacidolysis, followed by desulphuration, of jute fibers, and subsequent recyclization of the reaction β-β′ intermediates between C-α and C-3, as described by Lapierre et al. (*19*).

The relative proportions of the different types of condensed dimers in the jute MWL is shown in **Table 5**. Compounds with β-β′ tetralin and β-5′ structures were the most prominent thioacidolysis dimers released from jute MWL, accounting for 36 and 24% of the total identified dimers, respectively. The high proportion of β-β′ dimers (tetralin-type) was in agreement with the high amounts of β-β′ resinol substructures observed in jute lignin by 2D-NMR. More interestingly, most of the β-β′ dimers from the jute lignin were of the syringaresinol type, pinoresinol being completely absent, and the G-S resinol structure appearing in lower abundance (**Table 5**). The almost exclusive occurrence in jute lignin of β-β′ dimeric structures released from syringaresinol, together with the lack of pinoresinol-derived structures, was also observed in eucalypt wood (*16*).

β-1′ dimers were also present, although in lower amounts, in jute MWL. The existence of β-1′ dimeric substructures in lignin has been a matter of controversy for years. Recently, two β-1′ linked substructures, spirodienones and phenylisochromans, were identified using 2D-NMR in combination with DFRC (derivatization followed by reductive cleavage) (*40*−*42*). Phenylisochromans are resistant toward thioacidolysis, therefore, only spirodienones could be at the origin of the β-1′ dimers observed here.

The three thioacidolysis dimeric types with the lowest abundance, that is, 5-5′, 4-*O*-5′, and isochroman structures, were not detected by NMR because the abundance of the original substructures was below the NMR detection level. Dibenzodioxocins are supposed to be the main biphenyl structures in lignin (*43*, *44*), therefore, the 5-5′ dimers were considered mostly as being

dibenzodioxocin degradation products, although simple biphenyl structures have also been reported in lignin (*11*, *45*). The isochroman structure is probably formed by side chain migration (from C1 to C6) of a spirodienone intermediate during lignin biosynthesis (*40*, *41*).

In addition to the above dimeric compounds, some thioacidolysis trimers were also identified. These trimeric compounds presented a molecular ion (and base peak) at *m*/*z* 696 and a fragment at *m*/*z* 306 (characteristic of *β*-*β*′ tetralin dimers of the syringaresinol type). The trimers were tentatively identified as being formed by addition to the *β*-*β*′ tetralin dimers previously described (compounds **21**, **23**, and **26**) of a G lignin unit linked by a 4-*O*-5′ ether bond (S-*β*-*β*′-S′-4′-*O*-5′′-G′′ trimers, **Figure 6**). Three isomers of this trimeric structure were detected, as also occurred with the corresponding dimers (**Figure 6**), that were among the main dimeric compounds released from jute lignin. The same thioacidolysis trimeric compounds have been previously identified in hardwoods (*16*, *46*), and the corresponding G-G-G trimer has been reported in spruce (*47*).

ACKNOWLEDGMENT

This study has been funded by the Spanish project AGL2005-01748 and the EU BIORENEW Project (NMP2-CT-2006-026456). J.R. thanks the Spanish CSIC for a I3P fellowship; G. M. thanks the Spanish Ministry of Education for a FPI fellowship. We finally thank J.M. Gras and G. Artal (CELESA, Spain) for providing the jute fibers.

LITERATURE CITED

(1) Islam, A.; Sarkanen, K. V. The isolation and characterization of the lignins of jute (*Corchorus capsularis*). *Holzforschung* **1993**, 47, 123–132.
(2) Akhtaruzzaman, A. F. M.; Shafi, M. Pulping of jute. *Tappi J.* **1995**, 78, 106–112.
(3) Jahan, M. S. Evaluation of additive in soda pulping of jute. *Tappi J.* **2001**, 84, 1–11.
(4) Jahan, M. S.; Al-Maruf, A.; Quaiyyum, M. A. Comparative studies of pulping of jute fiber, jute cutting and jute caddis. *Bangladesh J. Sci. Ind. Res.* **2007**, 42, 425–434.
(5) Jahan, M. S.; Kanna, G. H.; Mun, S. P.; Chowdhury, D. A. N. Variations in chemical characteristics and pulpability within jute plant (*Corchorus capsularis*). *Ind. Crops Prod.* **2008**, 28, 199–205.
(6) González-Vila, F. J.; Almendros, G.; del Río, J. C.; Martín, F.; Gutiérrez, A.; Romero, J. Ease of delignification assessment of wood from different Eucalyptus species by pyrolysis (TMAH)-GC/MS and CP/MAS ^{13}C-NMR spectroscopy. *J. Anal. Appl. Pyrol.* **1999**, 49, 295–305.
(7) del Río, J. C.; Gutiérrez, A.; Hernando, M.; Landín, P.; Romero, J.; Martínez, A. T. Determining the influence of eucalypt lignin composition in paper pulp yield using Py-GC/MS. *J. Anal. Appl. Pyrol.* **2005**, 74, 110–115.
(8) Faix, O.; Meier, D.; Fortmann, I. Thermal degradation products of wood. A collection of electron-impact (EI) mass spectra of monomeric lignin derived products. *Holz Roh-Werkst.* **1990**, 48, 351–354.
(9) Ralph, J.; Hatfield, R. D. Pyrolysis-GC/MS characterization of forage materials. *J. Agric. Food Chem.* **1991**, 39, 1426–1437.
(10) del Río, J. C.; Gutiérrez, A.; Martínez, A. T. Identifying acetylated lignin units in non-wood fibers using pyrolysis-gas chromatography/mass spectrometry. *Rapid Commun. Mass Spectrom.* **2004**, 18, 1181–1185.
(11) Capanema, E. A.; Balakshin, M. Y.; Kadla, J. F. A comprehensive approach for quantitative lignin characterization by NMR spectroscopy. *J. Agric. Food Chem.* **2004**, 52, 1850–1860.
(12) Capanema, E. A.; Balakshin, M. Y.; Kadla, J. F. Quantitative characterization of a hardwood milled wood lignin by nuclear magnetic resonance spectroscopy. *J. Agric. Food Chem.* **2005**, 53, 9639–9649.
(13) Liitiä, T. M.; Maunu, S. L.; Hortling, B.; Toikka, M.; Kilpeläinen, I. Analysis of technical lignins by two- and three-dimensional NMR spectroscopy. *J. Agric. Food Chem.* **2003**, 51, 2136–2143.
(14) Ralph, J.; Marita, J. M.; Ralph, S. A.; Hatfield, R. D.; Lu, F.; Ede, R. M.; Peng, J.; Quideau, S.; Helm, R. F.; Grabber, J. H.; Kim, H.; Jimenez-Monteon, G.; Zhang, Y.; Jung, H. -J. G.; Landucci, L. L.; MacKay, J. J.; Sederoff, R. R.; Chapple, C.; Boudet, A. M. Solution-state NMR of lignin. In *Advances in lignocellulosics characterization*; Argyropoulos, D. S., Ed.; Tappi Press: Atlanta, 1999; pp 55−108.
(15) Ralph, S. A.; Ralph, J.; Landucci, L. *NMR database of lignin and cell wall model compounds*; US Forest Prod. Lab.: One Gifford Pinchot Dr., Madison, WI 53705, 2004 (http://ars.usda.gov/Services/docs.htm?docid=10491; accessed: January, 2009).
(16) Rencoret, J.; Marques, G.; Gutiérrez, A.; Ibarra, D.; Li, J.; Gellerstedt, G.; Santos, J. I.; Jiménez-Barbero, J.; Martínez, A. T.; del Río, J. C. Structural characterization of milled wood lignin from different eucalypt species. *Holzforschung* **2008**, 62, 514–526.
(17) del Río, J. C.; Rencoret, J.; Marques, G.; Gutiérrez, A.; Ibarra, D.; Santos, J. I.; Jiménez-Barbero, J.; Zhang, L.; Martínez, A. T. Highly acylated (acetylated and/or *p*-coumaroylated) native lignins from diverse herbaceous plants. *J. Agric. Food Chem.* **2008**, 56, 9525–9534.
(18) Lapierre, C.; Pollet, B.; Monties, B. Thioacidolysis of spruce lignin: GC-MS analysis of the main dimers recovered after Raney nickel desulphuration. *Holzforschung* **1991**, 45, 61–68.
(19) Lapierre, C.; Pollet, B.; Rolando, C. New insights into the molecular architecture of hardwood lignins by chemical degradative methods. *Res. Chem. Intermed.* **1995**, 21, 397–412.
(20) Rolando, C.; Monties, B.; Lapierre, C. Thioacidolysis. In *Methods in lignin chemistry*; Lin, S. Y., , Dence, C. W., Eds.; Springer-Verlag: Berlin, 1992; pp 334−349.
(21) *Tappi Test Methods 2004−2005*; Tappi Press: Norcoss, GA, 2004.
(22) Björkman, A. Studies on finely divided wood. Part I. Extraction of lignin with neutral solvents. *Sven. Papperstidn.* **1956**, 59, 477–485.
(23) Martínez, A. T.; Rencoret, J.; Marques, G.; Gutiérrez, A.; Ibarra, D.; Jiménez-Barbero, J.; del Río, J. C. Monolignol acylation and lignin structure in some nonwoody plants: A 2D-NMR study. *Phytochemistry* **2008**, 69, 2831–2843.
(24) Heikkinen, S.; Toikka, M. M.; Karhunen, P. T.; Kilpeläinen, I. A. Quantitative 2D HSQC (Q-HSQC) via suppression of *J*-dependence of polarization transfer in NMR spectroscopy: Application to wood lignin. *J. Am. Chem. Soc.* **2003**, 125, 4362–4367.
(25) Zhang, L. M.; Gellerstedt, G. Quantitative 2D HSQC NMR determination of polymer structures by selecting suitable internal standard references. *Magn. Reson. Chem.* **2007**, 45, 37–45.
(26) McDougall, G. J.; Morrison, I. M.; Stewart, D.; Weyers, J. D. B.; Hillman, J. R. Plant fibres: Botany, chemistry and processing for industrial use. *J. Sci. Food Agric.* **1993**, 62, 1–20.
(27) Moore, G. *Nonwood Fibre Applications in Papermaking*; Pira International, Leatherhead: Surrey, UK, 1996
(28) Lewin, M.; Pearce, E. M. *Handbook of fiber chemistry*; Marcel Dekker, Inc.: New York, 1998.
(29) Gutiérrez, A.; Rodríguez, I. M.; del Río, J. C. Chemical characterization of lignin and lipid fractions in industrial hemp bast fibers used for manufacturing high-quality paper pulps. *J. Agric. Food Chem.* **2006**, 54, 2138–2144.
(30) Gutiérrez, A.; Rodríguez, I. M.; del Río, J. C. Chemical characterization of lignin and lipid fractions in kenaf bast fibers used for manufacturing high-quality papers. *J. Agric. Food Chem.* **2004**, 52, 4764–4773.
(31) Rencoret, J.; Gutiérrez, A.; del Río, J. C. Lipid and lignin composition of woods from different eucalypt species. *Holzforschung* **2007**, 61, 165–174.
(32) Chang, H.-M.; Sarkanen, K. V. Species variation in lignin. Effect of species on the rate of kraft delignification. *Tappi* **1973**, 56, 132–134.
(33) Tsutsumi, Y.; Kondo, R.; Sakai, K.; Imamura, H. The difference of reactivity between syringyl lignin and guaiacyl lignin in alkaline systems. *Holzforschung* **1995**, 49, 423–428.
(34) Ralph, J.; Lu, F. The DFRC method for lignin analysis. 6. A simple modification for identifying natural acetates in lignin. *J. Agric. Food Chem.* **1998**, 46, 4616–4619.
(35) del Río, J. C.; Marques, G.; Rencoret, J.; Martínez, A. T.; Gutiérrez, A. Occurrence of naturally acetylated lignin units. *J. Agric. Food Chem.* **2007**, 55, 5461–5468.

(36) Brunow, G.; Karlsson, O.; Lundquist, K.; Sipilä, J. On the distribution of diastereomers of the structural elements in lignin: The steric course of reactions mimicking lignin biosynthesis. *Wood Sci. Technol*. **1993**, 27, 281–286.
(37) Akiyama, T.; Goto, H.; Nawawi, D.; Syafii, W.; Matsumoto, Y.; Meshitsuka, G. *Erythro*/*threo* ratio of β-O-4 structures as an important structural characteristic of lignin. Part 4: variation in the *erythro*/*threo* ratio in softwood and hardwood lignins and its relation to syringyl/guaiacyl ratio. *Holzforschung* **2005**, 59, 276–281.
(38) Kringstad, K. P.; Mörck, R. ^{13}C-NMR spectra of kraft lignins. *Holzforschung* **1983**, 37, 237–244.
(39) Ahvazi, B.; Argyropoulos, D. S. Thermodynamic parameters governing the stereoselective degradation of arylglycerol-β-aryl ether bonds in milled wood lignin under kraft pulping conditions. *Nordic Pulp Pap. Res. J*. **1997**, 12, 282–288.
(40) Ralph, J.; Peng, J. P.; Lu, F. C. Isochroman structures in lignin: a new β-1 pathway. *Tetrahedron Lett*. **1998**, 39, 4963–4964.
(41) Peng, J. P.; Lu, F. C.; Ralph, J. The DFRC method for lignin analysis - Part 5 - Isochroman lignin trimers from DFRC-degraded *Pinus taeda*. *Phytochemistry* **1999**, 50, 659–666.
(42) Zhang, L. M.; Gellerstedt, G. NMR observation of a new lignin structure, a spiro-dienone. *Chem. Commun*. **2001**, 2744–2745.
(43) Karhunen, P.; Rummakko, P.; Sipila, J.; Brunow, G.; Kilpeläinen, I. Dibenzodioxocins—A novel type of linkage in softwood lignins. *Tetrahedron Lett*. **1995**, 36, 169–170.
(44) Ralph, J.; Lundquist, K.; Brunow, G.; Lu, F.; Kim, H.; Schatz, P. F.; Marita, J. M.; Hatfield, R. D.; Ralph, S. A.; Christensen, J. H.; Boerjan, W. Lignins: Natural polymers from oxidative coupling of 4-hydroxyphenylpropanoids. *Phytochem. Rev*. **2004**, 3, 29–60.
(45) Balakshin, M. Y.; Capanema, E. A.; Goldfarb, B.; Frampton, J.; Kadla, J. F. NMR studies on Fraser fir *Abies fraseri* (Pursh) Poir. lignins. *Holzforschung* **2005**, 59, 488–496.
(46) Önnerud, H.; Gellerstedt, G. Inhomogeneities in the chemical structure of hardwood lignins. *Holzforschung* **2003**, 57, 255–265.
(47) Önnerud, H. Lignin structures in normal and compression wood. Evaluation by thioacidolysis using ethanethiol and methanethiol. *Holzforschung* **2003**, 57, 377–384.

Received March 11, 2009. Revised manuscript received August 18, 2009. Accepted September 28, 2009.